

# Variational method for non-conservative instability of a cantilever SWCNT in the presence of variable mass or crack

M.A. De Rosa

*School of Engineering, University of Basilicata, Viale dell'Ateneo Lucano 10, 85100  
Potenza, Italy*

M. Lippiello

*Department of Structures for Engineering and Architecture, University of Naples  
"Federico II", Via Forno Vecchio 36, 80134 Napoli, Italy*

N.M. Auciello

*School of Engineering, University of Basilicata, Viale dell'Ateneo Lucano 10, 85100  
Potenza, Italy*

H.D. Martin

*Facultad Regional Reconquista Universidad Tecnológica Nacional, Parque Industrial  
Reconquista, Calle 44 1000, S3560 Reconquista, Santa Fe, Argentina*

M.T. Piovan

*Centro de investigaciones de Mecánica Teórica y Aplicada, Universidad Tecnológica  
Nacional FRBB., 11 de Abril 461, B8000LMI, Bahía Blanca, Argentina*

---

## Abstract

In the present paper the non-conservative instability of a cantilever single-walled carbon nanotube (SWCNT) through nonlocal theory is investigated. The nanotube is modeled as clamped-free beam carrying a concentrated

---

*Email addresses:* [maria.derosa@unibas.it](mailto:maria.derosa@unibas.it) (M.A. De Rosa),  
[maria.lippiello@unina.it](mailto:maria.lippiello@unina.it) (M. Lippiello), [nicola.auciello@unibas.it](mailto:nicola.auciello@unibas.it) (N.M.  
Auciello), [hectordmartin@gmail.com](mailto:hectordmartin@gmail.com) (H.D. Martin), [mpiovan@frbb.utn.edu.ar](mailto:mpiovan@frbb.utn.edu.ar) (M.T.  
Piovan)

mass, located at a generic position, or in presence of a crack, and subjected to an axial load, at the free end. Nonlocal Euler-Bernoulli beam theory is used in the formulation and the governing equations of motion and the corresponding boundary conditions are derived using an extended Hamilton's variational principle. The governing equations are solved analytically. In order to show the sensitivity of the SWCNT to the values of an added mass, or crack and the influence of the nonlocal parameter and nondimensional crack severity coefficient on the fundamental frequencies values, some numerical examples have been performed and discussed. Also, the validity and the accuracy of the proposed analysis have been confirmed by comparing the results with those obtained from the literature.

*Keywords:* non-conservative instability, nonlocal elasticity, nanosensor, crack, variational method.

---

## 1. Introduction

Carbon nanotubes (CNTs) play a key role in a variety of engineering fields due to their superior mechanical, physical and electronic properties ([1]-[3]). Owing to these properties, CNTs have met applications in the emerging field of nanoelectronics, nanosensors, nanocomposites, bio-nanocomposites and so on ([4]-[6]). According to literature, the nanoscale of these structures suggests an atomistic model, but this approach turns out to be very expensive. On the other hand, although the classical continuum theories (Euler-Bernoulli, Timoshenko, or even higher-order theories) are able to predict the behaviors of nanostructures, it is found to be inadequate because of ignoring the small size effects. Thus adopting the nonlocal elasticity theory, as developed by Eringen in ([7]-[8]), is usual.

The theory of nonlocal elasticity finds general application in the area of nanostructural study such as in nanorods, nanobeams, nanoplates, nanorings, carbon nanotubes, graphenes, nanoswitches and protein microtubules. Although initiated by the work of Eringen, the use of nonlocal elasticity for nanostructures was applied for the first time by Peddieson et al. [9]. They employed a nonlocal elasticity theory to develop a nonlocal cantilever Euler-Bernoulli beam model, used as an actuator in small scale systems. Further applications of the nonlocal theory have been employed in studying the buckling ([10]-[11]) and vibration problems, by applying Euler-Bernoulli and Timoshenko beam theories, in CNTs ([9]-[16]).

Recent literatures show an increased utilization of CNTs as nanomechanical resonators in atomic-scale mass sensor ([17]-[18]). The nano-sized mass sensors are based on the fact that the resonant frequency is sensitive to the resonator and the attached mass. The change of the attached mass on the resonator causes the resonant frequency to deviate from its original value. The key challenge in mass detection is the quantification of variations in the resonant frequencies due to the added masses. Recently, mass detection based on the resonating nanomechanical tools has been subject of a growing interest as for example in ([19]-[23]).

Although many researches of nanoscale sensors have been conducted, the above-mentioned works are focused on the absence of axial forces. In fact, axial force or generalized follower force arises in practical applications due to initial stress, heat effect, end constraint, etc. ([24]-[25]). CNTs may be subjected to the follower force when they are utilized in different applications such as atomic force microscopy [26], scanning probe microscopy [27], nano-composites [28] and nano-pipes conveying fluid [29]. Thus, the stability analysis of CNT with non-conservative forces is important in designing nano-devices. In recent years, the influence of a non-conservative force on free-vibration of CNTs has attracted attention by many reseachers, although few papers can be found in literature regarding their structural stability. According to the nonlocal Euler-Bernoulli beam theory, Murmu and Pradhan [30] have analyzed the buckling analysis of single-walled carbon nanotube with effect of temperature change and surrounding elastic medium. Xiang et al. [31] have studied the dynamic instability phenomenon of cantilever nanotubes/nanorods under a follower force. Applying the Galerkin approach, Kazemi-Lari et al. [32] have investigated the influence of viscoelastic foundation on the non-conservative instability of the cantilever CNTs under a concentrated follower force. More recently, using the extended Hamilton's principle and the extended Galerkin's method, Kazemi-Lari et al. [33] have predicted the static and dynamic structural instability of CNTs subjected to a distributed tangential compressive load. Also, Bahaadini and Hosseini in [34] have investigated the nonlocal divergence and flutter instability analysis of CNTs conveying fluid embedded in elastic foundation under magnetic field. Finally, in [35] they have investigated the effects of nonlocal elasticity and slip condition on free vibration and flutter instability analysis of viscoelastic cantilever CNTs conveying fluid.

Further applications of the nonlocal elasticity theory have been employed in investigating buckling and vibrations problems in cracked CNTs. It is well

known that the presence of cracks in a structural member, such as nanotubes and nanobeams, introduces local flexibility and gives rise a local change in stiffness that may have significant influence on natural frequencies and mode shapes. With regards to the importance of the influence of crack effects on mechanical behaviours of nanostructures and thanks to their great theoretical and practical interest, an increasing interest has been devoted to the study of nanotubes with cracks ([36]-[41]). Loya et al. in [36] used the nonlocal Euler-Bernoulli beam theory to analyze the flexural vibrations of cracked micro- and nanobeams and to evaluate the effect of crack hardness, the nonlocal parameter and boundary conditions on natural frequencies of the cracked nanobeam. In their study the nanobeam is separated into two parts and the crack is simulated by a rotational spring. Joshi et al. in [37] have used an extended finite element method to simulate crack propagation in carbon nanotubes. Applying the nonlocal Euler-Bernoulli beam theory, Hsu et al. [38] have studied the longitudinal frequency of a cracked nanobeam for different boundary conditions and the influence of the crack parameter, crack location, and nonlocal parameter on the longitudinal frequency have investigated. Torabi and Dastgerdi [39] have investigated the free vibration of a cracked nanobeam modeled via nonlocal elasticity and Timoshenko beam theory. Their cracked nanobeam model is represented by two segments connected by a rotational spring. In [40] Hossein et al. have studied the axial vibration of a cracked nanorod in an elastic foundation based on nonlocal elasticity under different boundary conditions. In their paper, the cracked nanorod is modeled as two segments connected by a linear spring which is located at the cracked section. Loghmani and Yazdi in [41] dealt with the vibration analysis of multi cracked, stepped nanobeams by using wave approach and have discussed the effects of crack severity, crack and step location, mass of buckyball and small-scale parameter on natural frequencies.

In the present paper the non-conservative instability of cantilever single-walled carbon nanotube (SWCNT) through nonlocal theory is investigated. The nanotube is modeled as clamped-free beam carrying a concentrated mass  $M$ , located at a generic position, or in presence of a crack, and subjected to an axial load  $p$ , at the free end. Nonlocal Euler-Bernoulli beam theory is used in the formulation and the governing equations of motion and the corresponding boundary conditions are derived using an extended Hamilton's variational principle. The governing equations are solved analytically. In order to show the sensitivity of the SWCNT to the values of an added mass,

or in presence of a crack, and the influence of a nonlocal parameter and the crack severity coefficient on the fundamental frequencies values, some numerical examples have been performed and discussed. Also, the validity and the accuracy of the proposed analysis have been confirmed by comparing the results with those obtained from the literature.

## 2. Nonlocal equations of motion and their formulation

Consider a cantilever nanotube with span  $L$ , cross sectional area  $A$ , second moment of area  $I$ , Young modulus  $E$  and mass density  $\rho$ . An attached concentrated mass is located at position  $z=\gamma L$ , where  $z$  is the spatial coordinate along the nanotube, and a non-conservative force  $p$  is applied at the free-end of the nanotube, as shown in Figure 1.

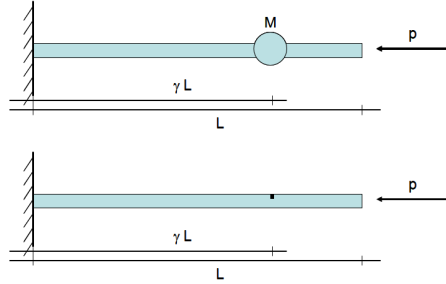


Figure 1: A cantilever single-walled nanotube with added mass at the generic position or in presence of crack.

According to Hamilton Principle it is possible to write:

$$\int_{t_1}^{t_2} (\delta T - \delta E_t) dt + \int_{t_1}^{t_2} \delta W_{nc} dt = 0 \quad (1)$$

with

$$T = \frac{1}{2} \int_0^{\gamma L} \rho A \left( \frac{\partial v_1(z, t)}{\partial t} \right)^2 dz + \frac{1}{2} \int_{\gamma L}^L \rho A \left( \frac{\partial v_2(z, t)}{\partial t} \right)^2 dz + \frac{1}{2} M \left( \frac{\partial v_1(\gamma L, t)}{\partial t} \right)^2 \quad (2)$$

$$\begin{aligned}
E_t = & \frac{1}{2} \int_0^{\gamma L} EI \left( \frac{\partial^2 v_1(z, t)}{\partial z^2} \right)^2 dz + \frac{1}{2} \int_{\gamma L}^L EI \left( \frac{\partial^2 v_2(z, t)}{\partial z^2} \right)^2 dz + \\
& - \int_0^L \left( (e_0 a)^2 \rho A \frac{\partial^2 v_1(z, t)}{\partial t^2} \right) \left( \frac{\partial^2 v_1(z, t)}{\partial z^2} \right) dz \\
& - \int_{\gamma L}^L \left( (e_0 a)^2 \rho A \frac{\partial^2 v_2(z, t)}{\partial t^2} \right) \left( \frac{\partial^2 v_2(z, t)}{\partial z^2} \right) dz - \frac{1}{2} \int_0^{\gamma L} p \left( \frac{\partial v_1}{\partial z} \right)^2 dz + \\
& - \frac{1}{2} \int_{\gamma L}^L p \left( \frac{\partial v_2}{\partial z} \right)^2 dz - \int_0^{\gamma L} \left( (e_0 a)^2 p \frac{\partial^2 v_1(z, t)}{\partial z^2} \right) \left( \frac{\partial^2 v_1(z, t)}{\partial z^2} \right) dz + \\
& - \int_{\gamma L}^L \left( (e_0 a)^2 p \frac{\partial^2 v_2(z, t)}{\partial z^2} \right) \left( \frac{\partial^2 v_2(z, t)}{\partial z^2} \right) dz + \frac{1}{2} k_c \left( \Delta \frac{\partial v(\gamma L, t)}{\partial z} \right)^2 \quad (3)
\end{aligned}$$

where  $T$  denotes the kinetic energy of the nanotube subjected to the concentrated mass  $M$ ,  $E_t$  is the total potential energy, sum of different contributions: the strain energy of the nanotube, the potential energy of the inertial force  $\left( \rho A \frac{\partial^2 v(z, t)}{\partial t^2} \right)$  due to the additional displacement  $\left( (e_0 a)^2 \frac{\partial^2 v(z, t)}{\partial z^2} \right)$ , the potential energy of the axial component of the nonconservative force and finally the potential energy of axial force due to the nonlocal parameter.

In Eq. (3),  $e_0$  is a constant, appropriate to each material, for calibrating the model with experimental results and other validated models: it is estimated such that the relations of the nonlocal elasticity model could provide satisfactory approximation to the atomic dispersion curves of the plane waves with those obtained from the atomistic lattice dynamics [42]. "a" is an internal (e.g. lattice parameter, granular size, distance between CC bonds) characteristic length of the nanostructure and  $k_c$  is the crack flexibility coefficient. Also, the work done by the transverse non-conservative axial force is considered:

$$\delta W_{nc} = -p \frac{\partial v_2(L, t)}{\partial z} \delta v_2(L, t) \quad (4)$$

The first variation of kinetic energy of the nanotube can be easily calcu-

lated as:

$$\begin{aligned} \delta T = & \int_0^{\gamma L} \rho A \frac{\partial v_1(z, t)}{\partial t} \delta \left( \frac{\partial v_1(z, t)}{\partial t} \right) dz + \\ & \int_{\gamma L}^L \rho A \frac{\partial v_2(z, t)}{\partial t} \delta \left( \frac{\partial v_2(z, t)}{\partial t} \right) dz + M \frac{\partial v_1(\gamma L, t)}{\partial t} \delta \left( \frac{\partial v_1(\gamma L, t)}{\partial t} \right) \end{aligned} \quad (5)$$

and the first variation of the potential energy is:

$$\begin{aligned} \delta E_t = & \int_0^{\gamma L} EI \frac{\partial^2 v_1(z, t)}{\partial z^2} \delta \frac{\partial^2 v_1(z, t)}{\partial z^2} dz - \int_0^{\gamma L} (e_0 a)^2 \rho A \frac{\partial^2 v_1(z, t)}{\partial t^2} \delta \frac{\partial^2 v_1(z, t)}{\partial z^2} dz + \\ & - \int_0^{\gamma L} p \frac{\partial v_1(z, t)}{\partial z} \delta \frac{\partial v_1(z, t)}{\partial z} dz - \int_0^{\gamma L} \left( (e_0 a)^2 p \frac{\partial^2 v_1(z, t)}{\partial z^2} \right) \delta \frac{\partial^2 v_1(z, t)}{\partial z^2} dz + \\ & \int_{\gamma L}^L EI \frac{\partial^2 v_2(z, t)}{\partial z^2} \delta \frac{\partial^2 v_2(z, t)}{\partial z^2} dz - \int_{\gamma L}^L (e_0 a)^2 \rho A \frac{\partial^2 v_2(z, t)}{\partial t^2} \delta \frac{\partial^2 v_2(z, t)}{\partial z^2} dz + \\ & - \int_{\gamma L}^L p \frac{\partial v_2(z, t)}{\partial z} \delta \frac{\partial v_2(z, t)}{\partial z} dz - \int_{\gamma L}^L \left( (e_0 a)^2 p \frac{\partial^2 v_2(z, t)}{\partial z^2} \right) \delta \frac{\partial^2 v_2(z, t)}{\partial z^2} dz + \\ & k_c \left( \frac{\partial v_2(\gamma L, t)}{\partial z} - \frac{\partial v_1(\gamma L, t)}{\partial z} \right) \left( \delta \frac{\partial v_2(\gamma L, t)}{\partial z} - \delta \frac{\partial v_1(\gamma L, t)}{\partial z} \right) \end{aligned} \quad (6)$$

Substituting Eqs (4-5) and (6) into Eq. (1), it assumes the following form:

$$\begin{aligned}
& \int_{t_1}^{t_2} [\delta T - \delta E_t + \delta W_{nc}] dt = \\
& \int_{t_1}^{t_2} \left[ \int_0^{\gamma L} \rho A \frac{\partial v_1(z, t)}{\partial t} \delta \frac{\partial v_1(z, t)}{\partial t} dz + \int_{\gamma L}^L \rho A \frac{\partial v_2(z, t)}{\partial t} \delta \frac{\partial v_2(z, t)}{\partial t} dz \right. \\
& - \int_0^{\gamma L} EI \frac{\partial^2 v_1(z, t)}{\partial z^2} \delta \frac{\partial^2 v_1(z, t)}{\partial z^2} dz + \int_0^{\gamma L} (e_0 a)^2 \rho A \frac{\partial^2 v_1(z, t)}{\partial t^2} \delta \frac{\partial^2 v_1(z, t)}{\partial z^2} dz + \\
& \int_0^{\gamma L} p \frac{\partial v_1(z, t)}{\partial z} \delta \frac{\partial v_1(z, t)}{\partial z} dz + \int_0^{\gamma L} (e_0 a)^2 p \frac{\partial^2 v_1(z, t)}{\partial z^2} \delta \frac{\partial^2 v_1(z, t)}{\partial z^2} dz + \\
& - \int_{\gamma L}^L EI \frac{\partial^2 v_2(z, t)}{\partial z^2} \delta \frac{\partial^2 v_2(z, t)}{\partial z^2} dz + \int_{\gamma L}^L (e_0 a)^2 \rho A \frac{\partial^2 v_2(z, t)}{\partial t^2} \delta \frac{\partial^2 v_2(z, t)}{\partial z^2} dz + \\
& \left. \int_{\gamma L}^L p \frac{\partial v_2(z, t)}{\partial z} \delta \frac{\partial v_2(z, t)}{\partial z} dz + \int_{\gamma L}^L (e_0 a)^2 p \frac{\partial^2 v_2(z, t)}{\partial z^2} \delta \frac{\partial^2 v_2(z, t)}{\partial z^2} dz \right. \\
& - p \frac{\partial v_2(L, t)}{\partial z} \delta v_2(L, t) + M \frac{\partial v_1(\gamma L, t)}{\partial t} \delta \frac{\partial v_1(\gamma L, t)}{\partial t} + \\
& \left. - k_c \left( \frac{\partial v_2(\gamma L, t)}{\partial z} - \frac{\partial v_1(\gamma L, t)}{\partial z} \right) \left( \delta \frac{\partial v_2(\gamma L, t)}{\partial z} - \delta \frac{\partial v_1(\gamma L, t)}{\partial z} \right) \right] dt \quad (7)
\end{aligned}$$

Performing integration by parts (see Appendix A), Eq. (7) becomes:

$$\begin{aligned}
& \int_{t_1}^{t_2} \left[ - \int_0^{\gamma L} \rho A \frac{\partial^2 v_1(z, t)}{\partial t^2} \delta v_1(z, t) dz - \int_{\gamma L}^L \rho A \frac{\partial^2 v_2(z, t)}{\partial t^2} \delta v_2(z, t) dz + \right. \\
& \int_0^{\gamma L} (-EI + (e_0 a)^2 p) \frac{\partial^4 v_1(z, t)}{\partial z^4} \delta v_1(z, t) dz + \int_{\gamma L}^L (-EI + (e_0 a)^2 p) \frac{\partial^4 v_2(z, t)}{\partial z^4} \delta v_2(z, t) dz + \\
& \int_0^{\gamma L} (e_0 a)^2 \rho A \frac{\partial^4 v_1(z, t)}{\partial t^2 \partial z^2} \delta v_1(z, t) dz + \int_{\gamma L}^L (e_0 a)^2 \rho A \frac{\partial^4 v_2(z, t)}{\partial t^2 \partial z^2} \delta v_2(z, t) dz \\
& \left. - \int_0^{\gamma L} p \frac{\partial^2 v_1(z, t)}{\partial z^2} \delta v_1(z, t) dz - \int_{\gamma L}^L p \frac{\partial^2 v_2(z, t)}{\partial z^2} \delta v_2(z, t) dz = 0 \right. \quad (8)
\end{aligned}$$



$$\begin{aligned}
& \int_{t_1}^{t_2} \left( \left[ (e_0 a)^2 \rho A \frac{\partial^2 v_1(z, t)}{\partial t^2} \delta \frac{\partial v_1(z, t)}{\partial z} \right]_0^{\gamma L} + \right. \\
& \left[ (e_0 a)^2 \rho A \frac{\partial^2 v_2(z, t)}{\partial t^2} \delta \frac{\partial v_2(z, t)}{\partial z} \right]_{\gamma L}^L - \left[ (e_0 a)^2 \rho A \frac{\partial^3 v_1(z, t)}{\partial t^2 \partial z} \delta v_1(z, t) \right]_0^{\gamma L} \\
& - \left[ (e_0 a)^2 \rho A \frac{\partial^3 v_2(z, t)}{\partial t^2 \partial z} \delta v_2(z, t) \right]_{\gamma L}^L + \left[ (-EI + (e_0 a)^2 p) \frac{\partial^2 v_1(z, t)}{\partial z^2} \delta \frac{\partial v_1(z, t)}{\partial z} \right]_0^{\gamma L} + \\
& \left[ (-EI + (e_0 a)^2 p) \frac{\partial^2 v_2(z, t)}{\partial z^2} \delta \frac{\partial v_2(z, t)}{\partial z} \right]_{\gamma L}^L - \left[ (-EI + (e_0 a)^2 p) \frac{\partial^3 v_1(z, t)}{\partial z^3} \delta v_1(z, t) \right]_0^{\gamma L} \\
& - \left[ (-EI + (e_0 a)^2 p) \frac{\partial^3 v_2(z, t)}{\partial z^3} \delta v_2(z, t) \right]_{\gamma L}^L + \left[ p \frac{\partial v_1(z, t)}{\partial z} \delta v_1(z, t) \right]_0^{\gamma L} + \\
& \left[ p \frac{\partial v_2(z, t)}{\partial z} \delta v_2(z, t) \right]_{\gamma L}^L - p \frac{\partial v_2(L, t)}{\partial z} \delta v_2(L, t) - M \frac{\partial^2 v_1(\gamma L, t)}{\partial t^2} \delta v_1(\gamma L, t) \\
& + k_c \left( \frac{\partial v_2(\gamma L, t)}{\partial z} - \frac{\partial v_1(\gamma L, t)}{\partial z} \right) \delta \frac{\partial v_1(\gamma L, t)}{\partial z} + \\
& - k_c \left( \frac{\partial v_2(\gamma L, t)}{\partial z} - \frac{\partial v_1(\gamma L, t)}{\partial z} \right) \delta \frac{\partial v_2(\gamma L, t)}{\partial z} \Big) dt = 0 \tag{9}
\end{aligned}$$

From Eq. (8), the governing equations of motion for a nanotube subjected to an axial load  $p$  and concentrated mass  $M$ , located at a generic position, can be derived as:

$$\begin{aligned}
& EI \frac{\partial^4 v_1(z, t)}{\partial z^4} + p \frac{\partial^2 v_1(z, t)}{\partial z^2} + \rho A \frac{\partial^2 v_1(z, t)}{\partial t^2} - \\
& (e_0 a)^2 \left( \rho A \frac{\partial^4 v_1(z, t)}{\partial t^2 \partial z^2} + p \frac{\partial^4 v_1(z, t)}{\partial z^4} \right) = 0, \quad 0 < z < \gamma L \tag{10}
\end{aligned}$$

$$\begin{aligned}
& EI \frac{\partial^4 v_2(z, t)}{\partial z^4} + p \frac{\partial^2 v_2(z, t)}{\partial z^2} + \rho A \frac{\partial^2 v_2(z, t)}{\partial t^2} - \\
& (e_0 a)^2 \left( \rho A \frac{\partial^4 v_2(z, t)}{\partial t^2 \partial z^2} + p \frac{\partial^4 v_2(z, t)}{\partial z^4} \right) = 0 \quad \gamma L < z < L \tag{11}
\end{aligned}$$

in which  $v_1(z, t)$  is the transverse displacement along  $\gamma L$  and  $v_2(z, t)$  along

$(L-\gamma L)$ , respectively. It can be easily noted that the Eqs. (10-11) are entirely coincident by those obtained according to the nonlocal theory of [8].

The general corresponding boundary conditions are:

for  $z=0$

$$v_1(0, t) = 0; \quad \frac{\partial v_1(0, t)}{\partial z} = 0 \quad (12)$$

for  $z=\gamma L$  in the presence of mass:

$$\begin{aligned} v_1(\gamma L, t) &= v_2(\gamma L, t) \\ \frac{\partial v_1(\gamma L, t)}{\partial z} &= \frac{\partial v_2(\gamma L, t)}{\partial z} \\ - (e_0 a)^2 \rho A \frac{\partial^3 v_1(\gamma L, t)}{\partial t^2 \partial z} - (-EI + (e_0 a)^2 p) \frac{\partial^3 v_1(\gamma L, t)}{\partial z^3} + \\ p \frac{\partial v_1(\gamma L, t)}{\partial z} - M \frac{\partial^2 v_1(\gamma L, t)}{\partial t^2} + (e_0 a)^2 \rho A \frac{\partial^3 v_2(\gamma L, t)}{\partial t^2 \partial z} + \\ (-EI + (e_0 a)^2 p) \frac{\partial^3 v_2(\gamma L, t)}{\partial z^3} - p \frac{\partial v_2(\gamma L, t)}{\partial z} &= 0; \end{aligned} \quad (13)$$

$$\begin{aligned} - (e_0 a)^2 \rho A \frac{\partial^2 v_1(\gamma L, t)}{\partial t^2} - (-EI + (e_0 a)^2 p) \frac{\partial^2 v_1(\gamma L, t)}{\partial z^2} + \\ (e_0 a)^2 \rho A \frac{\partial^2 v_2(\gamma L, t)}{\partial t^2} + (-EI + (e_0 a)^2 p) \frac{\partial^2 v_2(\gamma L, t)}{\partial z^2} &= 0 \end{aligned}$$

for  $z=\gamma L$  in the presence of crack:

$$\begin{aligned} v_1(\gamma L, t) &= v_2(\gamma L, t) \\ - k_c \left( \frac{\partial v_1(\gamma L, t)}{\partial z} - \frac{\partial v_2(\gamma L, t)}{\partial z} \right) + \\ (e_0 a)^2 \rho A \frac{\partial^2 v_1(\gamma L, t)}{\partial t^2} + (-EI + (e_0 a)^2 p) \frac{\partial^2 v_1(\gamma L, t)}{\partial z^2} &= 0 \end{aligned}$$

$$\begin{aligned}
& - (e_0a)^2 \rho A \frac{\partial^3 v_1(\gamma L, t)}{\partial t^2 \partial z} - (-EI + (e_0a)^2 p) \frac{\partial^3 v_1(\gamma L, t)}{\partial z^3} + \\
& p \frac{\partial v_1(\gamma L, t)}{\partial z} + (e_0a)^2 \rho A \frac{\partial^3 v_2(\gamma L, t)}{\partial t^2 \partial z} + \\
& (-EI (e_0a)^2 p) \frac{\partial^3 v_2(\gamma L, t)}{\partial z^3} - p \frac{\partial v_2(\gamma L, t)}{\partial z} = 0; \tag{14}
\end{aligned}$$

$$\begin{aligned}
& - (e_0a)^2 \rho A \frac{\partial^2 v_1(\gamma L, t)}{\partial t^2} - (-EI (e_0a)^2 p) \frac{\partial^2 v_1(\gamma L, t)}{\partial z^2} + \\
& (e_0a)^2 \rho A \frac{\partial^2 v_2(\gamma L, t)}{\partial t^2} + (-EI + (e_0a)^2 p) \frac{\partial^2 v_2(\gamma L, t)}{\partial z^2} = 0
\end{aligned}$$

and for  $z=L$ :

$$\begin{aligned}
& - (e_0a)^2 \rho A \frac{\partial^3 v_2(L, t)}{\partial t^2 \partial z} - (-EI + (e_0a)^2 p) \frac{\partial^3 v_2(L, t)}{\partial z^3} = 0; \\
& (e_0a)^2 \rho A \frac{\partial^2 v_2(L, t)}{\partial t^2} + (-EI + (e_0a)^2 p) \frac{\partial^2 v_2(L, t)}{\partial z^2} = 0 \tag{15}
\end{aligned}$$

The method of variables separation can be applied, so that the solution for Eqs (10-11) can be assumed as:

$$v_j(z, t) = v_j(z) e^{i\omega t} \quad j = 1, 2 \tag{16}$$

which if inserted into the Eqs (10-11) and if the nondimensional abscissa  $\zeta = \frac{z}{L}$  is introduced, the equations of motion assume the following form:

$$\begin{aligned}
& \frac{\partial^4 v_1(\zeta)}{\partial \zeta^4} + \frac{pL^2}{EI} \frac{\partial^2 v_1(\zeta)}{\partial \zeta^2} - \frac{\omega^2 \rho AL^4}{EI} v_1(\zeta) - \\
& (e_0a)^2 \left( -\frac{\omega^2 \rho AL^2}{EI} \frac{\partial^2 v_1(\zeta)}{\partial \zeta^2} + \frac{p}{EI} \frac{\partial^4 v_1(\zeta)}{\partial \zeta^4} \right) = 0, \quad 0 < \zeta < \gamma \\
& \frac{\partial^4 v_2(\zeta)}{\partial \zeta^4} + \frac{pL^2}{EI} \frac{\partial^2 v_2(\zeta)}{\partial \zeta^2} - \frac{\omega^2 \rho AL^4}{EI} v_2(\zeta) - \\
& (e_0a)^2 \left( -\frac{\omega^2 \rho AL^2}{EI} \frac{\partial^2 v_2(\zeta)}{\partial \zeta^2} + \frac{p}{EI} \frac{\partial^4 v_2(\zeta)}{\partial \zeta^4} \right) = 0, \quad \gamma < \zeta < 1 \tag{17}
\end{aligned}$$

For convenience of analysis, the following nondimensional terms are also introduced:

$$\eta = \frac{(e_0 a)}{L}; \quad P^2 = \frac{pL^2}{EI}; \quad \Omega = \sqrt[4]{\frac{\omega^2 \rho AL^4}{EI}} \quad (18)$$

and if denoting:

$$q = (1 - \eta^2 P^2); \quad r = (\eta^2 \Omega^4 + P^2) \quad (19)$$

Eq. (17) becomes:

$$\begin{aligned} q \frac{\partial^4 v_1(\zeta)}{\partial \zeta^4} + r \frac{\partial^2 v_1(\zeta)}{\partial \zeta^2} - \Omega^4 v_1(\zeta) &= 0 \\ q \frac{\partial^4 v_2(\zeta)}{\partial \zeta^4} + r \frac{\partial^2 v_2(\zeta)}{\partial \zeta^2} - \Omega^4 v_2(\zeta) &= 0 \end{aligned} \quad (20)$$

and the corresponding boundary conditions turn into:

$$v_1(0) = 0; \quad \frac{\partial v_1(0)}{\partial \zeta} = 0; \quad (21)$$

in the presence of mass become:

$$\begin{aligned} v_1(\gamma) &= v_2(\gamma) \\ \frac{\partial v_1(\gamma)}{\partial \zeta} &= \frac{\partial v_2(\gamma)}{\partial \zeta} \\ r \frac{\partial v_1(\gamma)}{\partial \zeta} + q \frac{\partial^3 v_1(\gamma)}{\partial \zeta^3} + \Omega^4 M_s v_1(\gamma) - r \frac{\partial v_2(\gamma)}{\partial \zeta} - q \frac{\partial^3 v_2(\gamma)}{\partial \zeta^3} &= 0; \\ \eta^2 \Omega^4 v_1(\gamma) + q \frac{\partial^2 v_1(\gamma)}{\partial \zeta^2} - \eta^2 \Omega^4 v_2(\gamma) - q \frac{\partial^2 v_2(\gamma)}{\partial \zeta^2} &= 0 \end{aligned} \quad (22)$$

in the presence of crack become:

$$\begin{aligned}
v_1(\gamma) &= v_2(\gamma); \\
\frac{\partial v_1}{\partial \zeta}(\gamma) - \frac{\partial v_2}{\partial \zeta}(\gamma) + \psi \left( q \frac{\partial^2 v_1(\gamma)}{\partial \zeta^2} + \eta^2 \Omega^4 v_1(\gamma) \right) &= 0; \\
r \frac{\partial v_1(\gamma)}{\partial \zeta} + q \frac{\partial^3 v_1(\gamma)}{\partial \zeta^3} - r \frac{\partial v_2(\gamma)}{\partial \zeta} - q \frac{\partial^3 v_2(\gamma)}{\partial \zeta^3} &= 0 \\
\eta^2 \Omega^4 v_1(\gamma) + q \frac{\partial^2 v_1(\gamma)}{\partial \zeta^2} - \eta^2 \Omega^4 v_2(\gamma) - q \frac{\partial^2 v_2(\gamma)}{\partial \zeta^2} &= 0
\end{aligned} \tag{23}$$

At the right end the boundary conditions become:

$$\begin{aligned}
\left( q \frac{\partial^3 v_2(1)}{\partial \zeta^3} + \eta^2 \Omega^4 \frac{\partial v_2(1)}{\partial \zeta} \right) &= 0 \\
\left( q \frac{\partial^2 v_2(1)}{\partial \zeta^2} + \eta^2 \Omega^4 v_2(1) \right) &= 0
\end{aligned} \tag{24}$$

in which

$$M_s = \frac{M}{\rho A L}; \quad \Psi = \frac{EI}{k_c L} \tag{25}$$

A general solution of the differential equations system can be expressed as:

$$v_1(z) = C_1 \text{Cos}(\alpha \zeta) + C_2 \text{Sin}(\alpha \zeta) + C_3 \text{Cosh}(\beta \zeta) + C_4 \text{Sinh}(\beta \zeta) \tag{26}$$

$$v_2(z) = C_5 \text{Cos}(\alpha \zeta) + C_6 \text{Sin}(\alpha \zeta) + C_7 \text{Cosh}(\beta \zeta) + C_8 \text{Sinh}(\beta \zeta) \tag{27}$$

where  $C_j(j=1\dots 8)$  are unknown arbitrary constants and with

$$\alpha = \sqrt{\frac{1}{2q} \left( r + \sqrt{r^2 + 4q\Omega^4} \right)}; \quad \beta = \sqrt{\frac{1}{2q} \left( -r + \sqrt{r^2 + 4q\Omega^4} \right)}; \tag{28}$$

Since the above system of equations has a non-trivial solution, the determinant of the coefficient matrix should be zero.

### 3. Numerical examples: results and discussion

In this section, a comparative analysis is carried out to investigate the influence of various parameters on the instability behaviour of a cantilever single-walled carbon nanotube with concentrated mass  $M$  or in presence of crack and subjected to non-conservative axial load  $p$ . In order to ensure about the exactness of the numerical calculations and the accuracy of the proposed analysis, the obtained results are compared with those of available works in literature. Several comparison analyses are conducted to demonstrate the influence of the small-scale effect, the critical load, nondimensional attached mass and the crack severity parameter on the nondimensional frequency values of single-walled nanotube. The numerical results are presented in the form of tables and figures using the values for physical parameters of the SWCNT displayed in Table 1.

SWCNT properties	Symbol	Value	Unit
Density	$\rho$	1330	Kg/m <sup>3</sup>
Radius	R	0.68 10 <sup>-9</sup>	m
Cross section area	A	1.024 10 <sup>-18</sup>	m <sup>2</sup>
Moment of inertia	I	2.134 10 <sup>-37</sup>	m <sup>4</sup>
Young's modulus	E	1054 10 <sup>9</sup>	Pa
Length	L	20.7 10 <sup>-9</sup>	m

Table 1: Values for physical parameters of cantilever single-walled nanotube [20].

#### 3.1. Effect of nonlocal parameter and nondimensional critical load $P$ .

The small length scale factor  $e_0a$  plays a crucial role on the dynamic properties of nanotubes, even if its interpretation seems still to be an open question. Different values of nonlocal parameter  $e_0a$  for CNT have been reported by many researchers, for example, according to nonlocal beam theory, the value  $e_0 = 0.39$  was given by Eringen in [7], whereas Wang and Hu [43] proposed the value  $e_0=0.288$ . On the other hand, by using the nonlocal thin shell model and matching the theoretical buckling strains with those computed from molecular simulations, Zhang et al. [44] showed that the value of  $e_0$  is equal to 0.117. Finally, Xiang et al. in [31] have found that about 43% of reduction of the critical follower force can be realized for a nanorod with the length of about 10 nm when the scale factor  $\eta=e_0a/L$  reaches 0.2. Such reduction of the critical follower force shows the significant length scale

effect of nanomaterials on the flutter problem.

In this paper, a range of dimensionless nonlocal coefficient  $0 \leq e_0 a \leq 2.0$  is used for the analysis. Effect of the nonlocal parameter,  $\eta = e_0 a / L$ , on the natural frequencies of cantilever nanotube with attached mass  $M$ , located at the position  $z = \gamma L$ , is analyzed and two numerical examples have been performed. The first numerical example gives a comparison between the present results with those obtained in [31]. For different values of the nondimensional small-scale coefficient  $\eta$  [0, 0.01, 0.02, 0.1, 0.2] and nondimensional critical load factor  $\Lambda = P^2 / \pi^2 = [0, 0.5, 1, 2]$ , the first two nondimensional frequencies  $\Omega_1$  and  $\Omega_2$  have been calculated and the corresponding values have been reported in Table 2. As can be easily observed, the results are coincident and they show that with increasing the nonlocal effect, the critical load value of non-conservative force decreases. As well-known in literature the cantilever CNT subjected to a non-conservative force loses its stability via flutter if the first two frequencies values are coincident, whereas the conservative system loses its stability via divergence if the first frequency reaches to 0 when the axial load increases.

The second numerical example deals with the numerical comparison between the present results with those obtained by [45], in which the results have been obtained by employing the Cell-Discretization Method (CDM). Consider the cantilever nanotube with a concentrated mass  $M$ , at the free-end. The analysis has been performed in the presence and in the absence of the nonlocal effect, as shown in Table 3. As can be easily observed, the results are in excellent agreement with the results given by in [45]. In addition, from Table 3 it can be seen that if the value of nondimensional concentrated mass  $M_s$  increases, the first nondimensional frequency value decreases, whereas when the nonlocal effect increases the first nondimensional value increases.

### *3.2. Effect of nondimensional mass $M_s$ for a fixed value of axial load ( $P=1$ ) and varying the nonlocal parameter $\eta$ .*

In order to illustrate the influence of the nondimensional mass  $M_s$  on the first nondimensional frequency  $\Omega_1$ , in the following numerical example the cantilever nanotube with the added mass, located at the left end so that  $\gamma = 1$ , has been considered. Fixing the axial load  $P = 1$ , varying the nondimensional mass coefficient between 0 and 1 and assuming the peculiar case in which  $M_s = 2$ , i.e. the added mass value is the double of the nanosensor, the first nondimensional frequency  $\Omega_1$  has been calculated. Table 4 shows the comparison between the results given by the exact procedure, so as de-

		[27]	Present	[27]	Present
$\eta$	$\Lambda=(P^2/\pi^2)$	$\lambda_1=\Omega_1^4/\pi^4$		$\lambda_2=\Omega_2^4/\pi^4$	
0	$\Lambda_{cr}=2.0316$	1.246	1.246	1.246	1.246
0.01	0	0.1269	0.1269	4.9777	4.9777
	0.5	0.1815	0.1816	4.2882	4.2882
	1.0	0.2716	0.2716	3.5566	3.5567
	2.0	1.0026	1.0027	1.5165	1.5166
	$\Lambda_{cr}=2.0277$	1.241	1.2411	1.241	1.2411
0.02	0	0.1270	0.1270	4.9579	4.9579
	0.5	0.1812	0.1812	4.2633	4.2634
	1.0	0.2708	0.2708	3.5267	3.5268
	2.0	1.0442	1.0442	1.4329	1.4330
	$\Lambda_{cr}=2.0160$	1.228	1.2350	1.228	1.2350
0.1	0	0.1280	0.1280	4.3902	4.3902
	0.5	0.1692	0.1693	3.5555	3.5556
	1.0	0.2465	0.2466	2.6778	2.6778
	$\Lambda_{cr}=1.7015$	0.892	0.8914	0.892	0.8914
0.2	0	0.1315	0.1315	3.1713	3.1713
	0.5	0.1337	0.1337	2.0908	2.0908
	1.0	0.2015	0.2016	0.9323	0.9327
	$\Lambda_{cr}=1.1390$	0.414	0.4135	0.414	0.4135

Table 2: Numerical comparison between the present results with those obtained by [31].

duced in the present paper, and those obtained by Rayleigh-Ritz (R-R) and Cell-Discretization Method (CDM) approximate methods given in [45], in the absence and presence of nonlocal effect. From Table 4, the following considerations can be made: a) If the concentrated mass value increases, the natural frequency values decrease; b) if the nonlocal effect increases, the natural frequency values decrease. Also, setting the small-scale parameter equal to  $\eta = 0, 0.1, 0.3$  and  $M_s = 2$ , the fundamental frequencies values are almost coincident.

### 3.3. Critical load values $P_{cr}$ varying the nonlocal coefficient $\eta$ and for $M_s = 0$

In this subsection, the effect of nonlocal parameter on the flutter instability of cantilever nanotube is investigated and the critical load values are calculated. Figure 2 shows the flutter frequency versus flutter load for dif-



-	$\eta=0$			$\eta=0.1$			$\eta=0.3$		
	$M_s$	Exact	[35]	CDM	Exact	[35]	CDM	Exact	[35]
0	1.9082	1.9082	1.9081	1.9033	1.9033	1.9033	1.8610	1.8610	1.8618
0.1	1.7575	1.7575	1.7575	1.7535	1.7535	1.7535	1.7192	1.7192	1.7197
0.2	1.6512	1.6512	1.6511	1.64762	1.6476	1.6476	1.6169	1.6169	1.6173
0.3	1.5705	1.5705	1.5704	1.5671	1.5671	1.5671	1.53549	1.5385	1.5388
0.4	1.5061	1.5061	1.5061	1.5029	1.5029	1.5029	1.4757	1.4757	1.4759
0.5	1.4531	1.4531	1.4530	1.4499	1.4499	1.4499	1.4238	1.4238	1.4240
0.6	1.4081	1.4081	1.4081	1.4052	1.4052	1.4051	1.3798	1.3798	1.3799
0.7	1.3694	1.3694	1.3694	1.3665	1.3665	1.3665	1.3418	1.3418	1.3419
0.8	1.3354	1.3354	1.3354	1.3326	1.3326	1.3326	1.3085	1.3085	1.3087
0.9	1.3053	1.3053	1.3052	1.3025	1.3025	1.3025	1.2790	1.2790	1.2791
1.0	1.2782	1.2782	1.2782	1.2755	1.2755	1.2755	1.2525	1.2526	1.2526
1.1	1.2538	1.2538	1.2537	1.2511	1.2511	1.2511	1.2285	1.2285	1.2286
1.2	1.2315	1.2315	1.2315	1.2289	1.2289	1.2289	1.2066	1.2066	1.2067
1.3	1.2111	1.2119	1.2117	1.2085	1.2085	1.2085	1.1866	1.1866	1.1866
1.4	1.1922	1.1922	1.1922	1.1897	1.1897	1.1897	1.1681	1.1681	1.1681
1.5	1.1748	1.1748	1.1748	1.1722	1.1722	1.1722	1.1509	1.1509	1.1510
2	1.1030	1.1030	1.1030	1.1006	1.1007	1.1006	1.0806	1.0806	1.0806

Table 4: The first nondimensional frequency values for different values of nonlocal coefficient  $\eta = 0, 0.1, 0.3$  and of the nondimensional mass  $M_s$  and for a fixed value of  $P=1$ .

$M_s$	$\eta = 0$	[45]	$\eta = 0.1$	[45]
0	1.8751	1.8751	1.8792	1.8792
0.1	1.7227	1.7227	1.7258	1.7258
0.2	1.6164	1.6164	1.6187	1.6187
0.3	1.6164	1.5361	1.5380	1.5380
0.4	1.4724	1.4724	1.4740	1.4740
0.5	1.4200	1.4200	1.4213	1.4213
0.6	1.3757	1.3757	1.3768	1.3768
0.7	1.3375	1.3375	1.3385	1.3385
0.8	1.3041	1.3041	1.3050	1.3050
0.9	1.2745	1.2745	1.2753	1.2753
1	1.2479	1.2479	1.2486	1.2486

Table 3: Numerical comparison between the present results with those obtained by [45].

ferent values of the nonlocal parameter  $\eta=0,0.1,0.3,0.5$  and the four curves describe the relation between the nonlocal parameter and the critical loads. For  $\eta = 0$ , the results show that the critical load value, corresponding to the higher curve, is equal to  $P_{cr}^2=20.051$ . This value correspond to Beck's column solution so as already demonstrated by Bolotin in [47]. In addition, from Figure 2 one can deduce that the increase of the nonlocal coefficient value involves the decrease in the critical loads values. In particular, for  $\eta=0.1$ , the critical load is equal to  $P_{cr}^2=16.7854$ ; for  $\eta=0.3$ ,  $P_{cr}^2=7.22$ , and for  $\eta=0.5$ ,  $P_{cr}^2=3.355$ , respectively. As can be easily observed, the increase of the nonlocal coefficient value results in a considerable reduction of the critical load values and the flutter curves have a more tilted pattern.

#### 3.4. Critical load values $P_{cr}$ varying the added mass position.

In this numerical example, the influence of an added mass on the flutter instability of the cantilever nanotube is investigated. For a nondimensional value of the added mass equal to  $M_s = 1$  and the nonlocal coefficient  $\eta=0.1$ , in Figure 3 the flutter loads and the flutter frequency is plotted, as function of the added mass positions,  $\gamma=0.2,0.5,1$ . From Figure 3, one sees that the higher critical load value is equal to  $P_{cr}^2=20.3401$ , for  $\gamma=0.2$ . The increase with the added mass position involves the decrease in the critical loads values: in particular, for  $\gamma=0.5$ ,  $P_{cr}^2=16.3054$ , and for  $\gamma=0.1$ ,  $P_{cr}^2=13.7641$ .

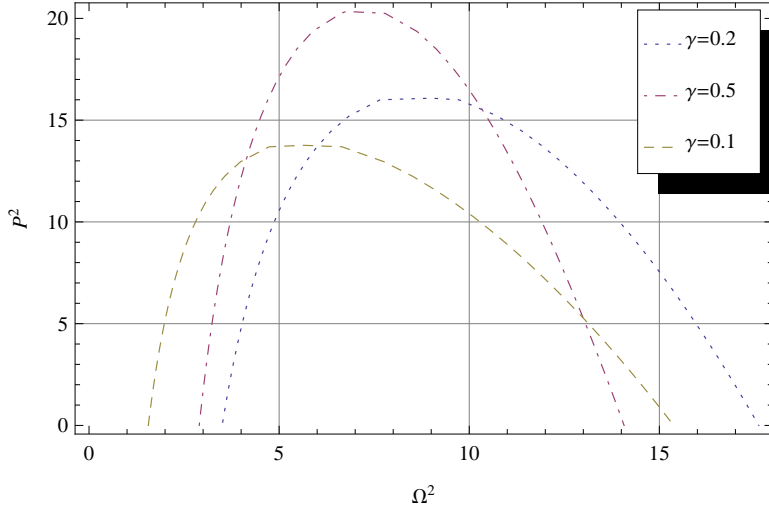


Figure 2: Flutter frequency versus flutter load for different values of nonlocal parameter,  $\eta=0,0.1,0.2,0.3,0.5$ .

### 3.5. Effect of nonlocal coefficient and crack severity parameter

In the following numerical example the case of a simply-supported nanotube with crack is considered and the influence of nonlocal coefficient and crack severity parameter on the non dimensional frequency is investigated. The crack is located at the nondimensional distance  $\gamma=0.5$  from the left end. Also, this numerical example deals with the numerical comparison between the present results with those obtained by Loya in [36].

Table 5 gives the changes of the first non dimensional four eigenvalues for different values of the crack severity  $\Psi= [0,0.065,0.35,2]$  and four different values of the nonlocal coefficient  $\eta$  equal to  $[0,0.2,0.4,0.6]$ .

From Table 5 can be easily observed that the non dimensional frequency values decrease with an increase of the crack severity coefficient and for a larger small scale parameter leads to a decrease of the crack effect on the vibration frequency. Also, as already observed by Loya in [36], due to the symmetry of the problem, the mid-span cracked nano-beam has the second and fourth natural frequencies independent of crack severity coefficient. Finally, as may be seen from Table 5, the first and third non dimensional frequencies values obtained by Loya in Table 1 of [36] are smaller than with the proposed approach. The difference between the results is due to the presence in the proposed variational approach of the non local effect in the

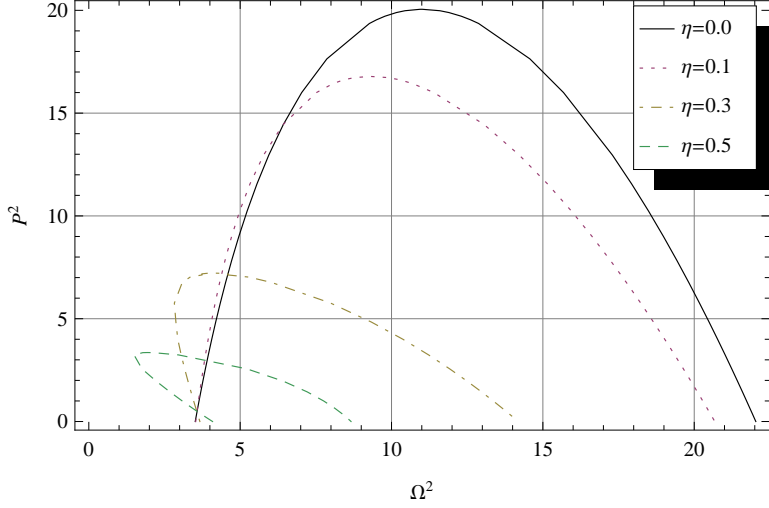


Figure 3: Flutter frequency versus flutter load for different values of added mass position  $\gamma=0.2,0.5,1$ .

boundary conditions of cracked nanotube (see the second Eq. 23). In particular, as can be seen, for an increase of the nonlocal effect value the first and third nondimensional frequency increase.

### 3.6. Critical loads values $P_{cr}$ varying the nonlocal coefficient $\eta$ and for nondimensional crack severity parameter $\Psi=1$

In the last numerical example the case of a clamped free nanotube with crack is considered and for the nondimensional crack severity parameter  $\Psi=1$  the influence of nonlocal coefficient on the flutter instability is investigated. The crack is located at  $\gamma=0.5$ . For a nondimensional value of the crack severity equal to  $\Psi = 1$ , in Figure 7 the flutter loads and the flutter frequency is plotted, as function of the nonlocal coefficient  $\eta=0.1$  and  $\eta=0.3$ . From Figure 7, one sees that the lower critical load value  $P_{cr}^2$  is equal to 4.7085, for  $\eta=0.3$ ; whereas for  $\eta=0.1$   $P_{cr}^2$  is equal to 6.7335.

Also, comparing the numerical results with those obtained for a clamped free nanotube in absence of crack and whose values are listed in Table 2, it can be easily observed that the influence of crack on the flutter instability are significant. In particular, as can be noted for  $\eta=0.1$ , the difference of critical load value  $P_{cr}^2$  for uncracked and cracked nanotubes is equal to 10.0519; whereas for  $\eta=0.3$   $P_{cr}^2(uncracked) - P_{cr}^2(cracked)$  is equal to 2.5115.

-	$\eta=0$				$\eta=0.2$			
	$\Psi=0$	$\Psi=0.065$	$\Psi=0.35$	$\Psi=2$	$\Psi=0$	$\Psi=0.065$	$\Psi=0.35$	$\Psi=2$
1	3.1416	3.0469	2.7496	2.0960	2.8908	2.8031	2.5233	1.9098
1	3.1416	3.0469	2.7496	2.0960	2.8908	2.8271	2.6103	2.0572
2	6.2832	6.2832	6.2832	6.2832	4.9581	4.9581	4.9581	4.9581
2	6.2832	6.2832	6.2832	6.2832	4.9581	4.9581	4.9581	4.9581
3	9.4248	9.1669	8.6129	8.6129	6.4520	6.2604	5.7891	5.3416
3	9.4248	9.1669	8.6129	8.6129	6.4520	6.4105	6.2956	6.1286
4	12.5664	12.5664	12.5664	12.5664	7.6407	7.6407	7.6407	7.6407
4	12.5664	12.5664	12.5664	12.5664	7.6407	7.6407	7.6407	7.6407
-	$\eta=0.4$				$\eta=0.6$			
	$\Psi=0$	$\Psi=0.065$	$\Psi=0.35$	$\Psi=2$	$\Psi=0$	$\Psi=0.065$	$\Psi=0.35$	$\Psi=2$
1	2.4790	2.4032	2.1567	1.6195	2.1507	2.0846	1.8678	1.3971
1	2.4790	2.4487	2.3342	1.9589	2.1507	2.1356	2.0750	1.8355
2	3.8204	3.8204	3.8204	3.8204	3.1815	3.1815	3.1815	3.1815
2	3.8204	3.8204	3.8204	3.8204	3.1815	3.1815	3.1815	3.1815
3	4.7723	4.6284	4.2729	3.9563	3.9329	3.8141	3.5526	3.2709
3	4.7723	4.7626	4.7304	4.6597	3.9329	3.9292	9.9152	3.8738
4	5.5509	5.5509	5.5509	5.5509	4.5566	4.5566	4.5566	4.5566
4	5.5509	5.5509	5.5509	5.5509	4.5566	4.5566	4.5566	4.5566

Table 6: The first four order frequency values for a simply-supported beam with different nonlocal parameter  $\eta$  and crack-severity  $\Psi$ . Crack position is  $\gamma = 0.50$ .

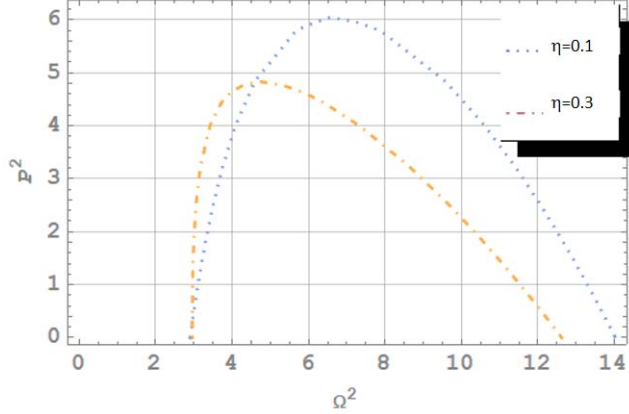


Figure 7: Flutter frequency versus flutter load for two different values of nonlocal parameter  $\eta=0.1$  and  $\eta=0.3$  and for crack severity coefficient  $\Psi=1$  .

#### 4. Concluding remarks

In the present paper, the dynamic instability of cantilever nanotube subjected to a non-conservative force, at the free end, and carrying an added mass, at a generic position, or in presence of a crack, has been investigated. In the first part of the present paper, the exact formulation of Hamilton Principle for a SWCNT, in the presence of nonlocal effect, non-conservative force, crack and concentrated mass is presented. Interestingly, this energy approach gives the same boundary problem as obtained by using the geometric method, given by [31]. Numerical comparisons have been performed in order to evaluate the effect of the nonlocal coefficient, the nondimensional crack severity parameter and nondimensional added mass. Taking into account the influence of the nonlocal parameter, the obtained results agrees with that observed by other authors, for the cantilever single-walled nanotube. If considers the presence of a crack, taking into account the influence of the nondimensional crack severity parameter, the obtained results agree with that observed by other authors, for the simply-supported single-walled nanotube. From the obtained results, it is observed that the influence of crack severity, nonlocal parameter and added mass on the vibration frequency of nanotubes are significant and, in particular, the following considerations ap-

- ply: a) if the nonlocal effect  $\eta$  increases and for the constant value of the nondimensional added mass  $M_s$ , the critical load value decreases;
- b) if the nondimensional added mass  $M_s$  increases and for the constant value of the non-conservative force, the natural frequency decreases; analogously, if the nonlocal effect value increases the fundamental frequency value decreases.
- c) if the nonlocal parameter  $\eta$  increases the critical load values decrease.
- d) the critical load values decrease as the added mass moves toward the free end of the nanotube.
- e) the nondimensional frequency decreases with an increase of the crack severity parameter;
- f) a larger small scale parameter leads to a decrease of the crack effect on the vibration frequency.

## References

- [1] Ruoff RS, Lorents DC. Mechanical and thermal properties of carbon nanotubes. *Carbon* 1995; 33: 925-30.
- [2] Jiang H, Liu B, Huang Y, Hwang KC. Thermal expansion of single wall carbon nanotubes. *J Mat. Tech. ASME* 2004; 126: 265-70.
- [3] Avouris P, Appenzeller J, Martel R, Wind SJ. Carbon Nanotube Electronics. *Proc. IEEE* 2003; 91: 1772-84.
- [4] Tsukagoshi K, Yoneya N, Uryu S, Aoyagi Y, Kanda A, Ootuka Y, Alphenaar BW. Carbon nanotube devices for nanoelectronics. *Physica B* 2002; 323: 107-14.
- [5] Lau KY, Chipara M, Ling HY, Hui D. Carbon nanotube devices for nanoelectronics. *Composites B* 2004; 35: 95-101.
- [6] An KH, Jeong SY, Hwang HR, Lee YH. Enhanced Sensitivity of a Gas Sensor Incorporating Single-Walled Carbon Nanotube-Polypyrrole Nanocomposites. *Adv. Mat.* 2004; 16 (12): 1005-09.
- [7] Eringen AC. On differential equations of non local elasticity and solutions of screw dislocation and surface-waves. *J. Appl. Phys.* 1983; 54: 4703-10.
- [8] Eringen AC. *Nonlocal continuum fields theories*. New York Springer-Verlag; 2002.

- [9] Peddieson J, Buchanan GR, McNitt RP. Application of nonlocal continuum models to nanotechnology. *Int. J. Eng. Sci.* 2003; 41: 305-312.
- [10] Ghannadpour SAM, Mohammadi B, Fazilati J. Bending buckling and vibration problems of nonlocal Euler beams using Ritz method, *Comp. Struct.* 2013 (96): 584-589.
- [11] Pradhan SC, Phadicar JK. Bending buckling and vibration analyses of nonhomogeneous nanotubes using GDQ and nonlocal elasticity theory, *Struct. Eng. and Mech. an Int. Journal* 2009; 33 (2): 193-213.
- [12] Wang Q, Varadan VK. Vibration of carbon nanotubes studied using nonlocal continuum mechanics, *Smart Materials and Structures* 2006; 15: 659-666.
- [13] De Rosa MA, Lippiello M. Free vibration analysis of DWCNTs using CDM and Rayleigh-Schmidt based on nonlocal Euler-Bernoulli beam theory. *The Scientific World Journal* 2014; 2014:1-12.
- [14] De Rosa MA, Lippiello M. Nonlocal frequency analysis of embedded single-walled carbon nanotube using the Differential Quadrature Method. *Comp. Part B Eng.* 2016; 84: 41-51.
- [15] De Rosa MA, Lippiello M. Nonlocal Timoshenko frequency analysis of single-walled carbon nanotube with attached mass: An alternative hamiltonian approach. *Comp. Part B Eng.* 2017; 111: 409-418.
- [16] Ansari R, Sahmani S. Small scale effect on vibrational response of single-walled carbon nanotubes with different boundary conditions based on nonlocal beam models. *Commun. Nonlinear Sci. Numer. Simulat.* 2012; 17: 1965-1979.
- [17] Lee HL, Hsu JC, Chang WJ. Frequency shift of carbon nanotube-based mass sensors using nonlocal elasticity theory. *Nanoscale Research Letters* 2010; 5: 1774-1778.
- [18] Aydogdu M, Filiz S. Modeling carbon nanotube-based mass sensors using axial vibration and nonlocal elasticity. *Physica E* 2001; 43: 1229-1234.



- [19] Murmu T, Adhikari S. Nonlocal frequency analysis of nanoscale biosensors. *Sensor and Actuators A* 2012; 173: 41-48.
- [20] Mehdipour I, Erfani - Moghadam A, Mehdipour C. Application of an electrostatically actuated cantilevered carbon nanotube with an attached mass as a bio-mass sensor. *Curr. Appl. Phys.* 2013; 13: 1463 - 1469.
- [21] De Rosa MA, Lippiello M. Hamilton principle for SWCN and a modified approach for nonlocal frequency analysis of nanoscale biosensor. *Int. J. of Recent Scient. Research (IJRSR)* 2015; 6 (1): 2355-65.
- [22] De Rosa MA, Lippiello M, Hector DM, Piovan MT. Nonlocal frequency analysis of nanosensors with different boundary conditions and attached distributed biomolecules: an approximate method. *Acta Mech.* 227 (8) 2016, 2323-2342; DOI 10.1007/s00707-016-1631-4.
- [23] Elishakoff I, Versaci C, Muscolino G. Clamped-Free double-walled carbon nanotube-based mass sensor. *Acta Mechanica* 2011; 219: 29-43.
- [24] De Rosa MA, Franciosi C. The influence of an intermediate support on the stability behaviour of cantilever beams subjected to follower forces. *J. of Sound and Vibration* 1990; 137(1): 107-115.
- [25] De Rosa MA, Lippiello M, Auciello NM. Dynamic stability analysis and DQM for beams with variable cross-section. *Mech. Res. Comm.* 2008; 35: 187-192.
- [26] Postma HWC, Sellmeijer A, Dekker C. Manipulation and Imaging of Individual Single-Walled Carbon Nanotubes with an Atomic Force Microscope. *Adv. Mater.* 2000; 12(17): 1299-1302.
- [27] Shen ZB, Deng B, Li XF, Tang GJ. Buckling Instability of Carbon Nanotube Atomic Force Microscope Probe Clamped in an Elastic Medium. *ASME J. Nanotechnol. Eng. Med.* 2011; 3 (2): 031003-07.
- [28] Suhir E. Elastic Stability of a Cantilever Beam (Rod) Supported by an Elastic Foundation, With Application to Nano-Composites. *J. of Appl. Mech.* 2012; 79: 011009-1.

- [29] Yoon J, Ru CQ, Mioduchowski A. Flow-induced flutter instability of cantilever carbon nanotubes. *Int. J. of Solids and Struct.* 2006; 43 (11-12): 3337-3349.
- [30] Murmu T, Pradhan SC. Thermal effects on the stability of embedded carbon nanotubes. *Comp. Mat. Science* 2010; 47: 721-726.
- [31] Xiang Y, Wang CM., Kitipornchai S, Wang Q. Dynamic Instability of nanorods/Nanotubes subjected to an End Follower Force. *J. of Eng. Mech. ASCE* 2010; 136(8): 1054-1058.
- [32] Kazemi-Lari MA, Fazelzadeh SA, Ghavanloo E. Non-conservative instability of cantilever carbon nanotubes resting on viscoelastic foundation. *Physica E* 2012; 44: 1623-1630.
- [33] Kazemi-Lari MA, Ghavanloo E, Fazelzadeh SA. Structural instability of carbon nanotubes embedded in viscoelastic medium and subjected to distributed tangential load. *J. of Mech, Sci. and Tech.* 2013; 27 (7): 2085-2091.
- [34] Bahaadini R, Hosseini M. Nonlocal divergence and flutter instability analysis of embedded fluid-conveying carbon nanotube under magnetic field. *Microfluid Nanofluid* 2016; 20(108): 1-14.
- [35] Bahaadini R, Hosseini M. Effects of nonlocal elasticity and slip condition on vibration and stability analysis of viscoelastic cantilever carbon nanotubes conveying fluid. *Comp. Mat. Scie.* 2016; 114: 151-159.
- [36] Loya J, López-Puente J, Zaera R, Fernández-Sáez J. Free transverse vibrations of cracked nanobeams using a nonlocal elasticity model. *J Appl Phys* 2009; 105:044309.
- [37] Joshi AY, Sharma SC, Harsha SP. Analysis of crack propagation in fixed-free singlewalled carbon nanotube under tensile loading using XFEM. *J Nanotechnol Eng Med* 2010; 1:041008.
- [38] Hsu JC, Lee HL, Chang WJ. Longitudinal vibration of cracked nanobeams using nonlocal elasticity theory. *Curr Appl Phys* 2011; 11:1384-8.

- [39] Torabi K, Nafar Dastgerdi J. An analytical method for free vibration analysis of Timoshenko beam theory applied to cracked nanobeams using a nonlocal elasticity model. *Thin Solid Films* 2012; 520:6595-602.
- [40] Hosseini AH, Rahmani O, Nikmehr M, Fakhari Golpayegani I. Axial vibration of cracked nanorods embedded in elastic foundation based on a nonlocal elasticity model. *Sens Lett* 2016; 14:1019-25.
- [41] Loghmani M, Yazdi MRH. An analytical method for free vibration of multi cracked and stepped nonlocal nanobeams based on wave approach. *Results in Physics* 2018; 11:166-181.
- [42] Murmu T, Adhikari S. Nonlocal effects in the longitudinal vibration of double-nanorod systems. *Physica E* 2010; 43: 415-422.
- [43] Wang LF, Hu HY. Flexural wave propagation in single-walled carbon nanotubes. *Phys. Rev. B* 2005; 71: 195412.
- [44] Zhang YQ, Liu GR, Xie XY. Free transverse vibrations of double -walled carbon nanotubes using a theory of nonlocal elasticity. *Phys. Rev. B* 2005; 71: 195404.
- [45] De Rosa MA, Lippiello M. Free vibration analysis of SWCNT using CDM in the presence of nonlocal effect. *Int.J. of Eng. and Inn. Tech. (IJEIT)* 2014; 4 (4):92-102.
- [46] De Rosa MA, Lippiello M, Auciello NM. Nonconservative instability of cantilevered nanotube via Cell Discretization Method. submitted to
- [47] Bolotin VV. *Nonconservative problems of the theory of elastic stability.* Pergamon press, 1963.

*Appendix A - Integration by parts and boundary conditions*

A series of integration by part can be conducted on the terms of Eq (7), leading to:

$$\int_0^{\gamma L} \left[ \int_{t_1}^{t_2} \rho A \frac{\partial v_1(z, t)}{\partial t} \delta \frac{\partial v_1(z, t)}{\partial t} dt \right] dz =$$

$$\int_0^{\gamma L} \left[ \rho A \frac{\partial v_1(z, t)}{\partial t} \delta v_1(z, t) \right]_{t_1}^{t_2} dz - \int_0^{\gamma L} \left[ \int_{t_1}^{t_2} \rho A \frac{\partial^2 v_1(z, t)}{\partial t^2} \delta v_1(z, t) dt \right] dz$$

$$\begin{aligned}
& \int_{\gamma L}^L \left[ \int_{t_1}^{t_2} \rho A \frac{\partial v_2(z, t)}{\partial t} \delta \frac{\partial v_2(z, t)}{\partial t} dt \right] dz = \\
& \int_{\gamma L}^{\gamma L} \left[ \rho A \frac{\partial v_2(z, t)}{\partial t} \delta v_2(z, t) \right]_{t_1}^{t_2} dz - \int_{\gamma L}^L \left[ \int_{t_1}^{t_2} \rho A \frac{\partial^2 v_2(z, t)}{\partial t^2} \delta v_2(z, t) dt \right] dz;
\end{aligned} \tag{A1}$$

and

$$\int_{t_1}^{t_2} M \frac{\partial v_1(\gamma L, t)}{\partial t} \delta \frac{\partial v_1(\gamma L, t)}{\partial t} dt = \left[ M \frac{\partial v_1(\gamma L, t)}{\partial t} \delta v_1(\gamma L, t) \right]_{t_1}^{t_2} - \int_{t_1}^{t_2} M \frac{\partial^2 v_2(\gamma L, t)}{\partial t^2} \delta v_2(\gamma L, t) dt; \tag{A2}$$

and

$$\begin{aligned}
& \int_{t_1}^{t_2} \left[ \int_0^{\gamma L} p \frac{\partial v_1(z, t)}{\partial z} \delta \frac{\partial v_1(z, t)}{\partial z} dz \right] dt = \\
& \int_{t_1}^{t_2} \left[ p \frac{\partial v_1(z, t)}{\partial z} \delta v_1(z, t) \right]_0^{\gamma L} dt - \left[ \int_0^{\gamma L} p \frac{\partial^2 v_1(z, t)}{\partial z^2} \delta v_1(z, t) dz \right] dt; \\
& \int_{t_1}^{t_2} \left[ \int_{\gamma L}^L p \frac{\partial v_2(z, t)}{\partial z} \delta \frac{\partial v_2(z, t)}{\partial z} dz \right] dt = \\
& \int_{t_1}^{t_2} \left[ p \frac{\partial v_2(z, t)}{\partial z} \delta v_2(z, t) \right]_{\gamma L}^L dt - \left[ \int_{\gamma L}^L p \frac{\partial^2 v_2(z, t)}{\partial z^2} \delta v_2(z, t) dz \right] dt; \tag{A3}
\end{aligned}$$

and

$$\begin{aligned}
& \int_{t_1}^{t_2} \left[ \int_0^{\gamma L} (-EI + (e_0 a)^2 p) \frac{\partial^2 v_1(z, t)}{\partial z^2} \delta \frac{\partial^2 v_1(z, t)}{\partial z^2} dz \right] dt = \\
& \int_{t_1}^{t_2} \left[ (-EI + (e_0 a)^2 p) \frac{\partial^2 v_1(z, t)}{\partial z^2} \delta \frac{\partial v_1(z, t)}{\partial z} \right]_0^{\gamma L} dt - \\
& \int_{t_1}^{t_2} \left[ \int_0^{\gamma L} (-EI + (e_0 a)^2 p) \frac{\partial^3 v_1(z, t)}{\partial z^3} \delta \frac{\partial v_1(z, t)}{\partial z} dz \right] dt = \\
& \int_{t_1}^{t_2} \left[ (-EI + (e_0 a)^2 p) \frac{\partial^2 v_1(z, t)}{\partial z^2} \delta \frac{\partial v_1(z, t)}{\partial z} \right]_0^{\gamma L} dt - \\
& \int_{t_1}^{t_2} \left[ (-EI + (e_0 a)^2 p) \frac{\partial^3 v_1(z, t)}{\partial z^3} \delta v_1(z, t) \right]_0^{\gamma L} dt + \\
& \int_{t_1}^{t_2} \left[ \int_0^{\gamma L} (-EI + (e_0 a)^2 p) \frac{\partial^4 v_1(z, t)}{\partial z^4} \delta v_1(z, t) dz \right] dt; \\
& \int_{t_1}^{t_2} \left[ \int_{\gamma L}^L (-EI + (e_0 a)^2 p) \frac{\partial^2 v_2(z, t)}{\partial z^2} \delta \frac{\partial^2 v_2(z, t)}{\partial z^2} dz \right] dt = \\
& \int_{t_1}^{t_2} \left[ (-EI + (e_0 a)^2 p) \frac{\partial^2 v_2(z, t)}{\partial z^2} \delta \frac{\partial v_2(z, t)}{\partial z} \right]_{\gamma L}^L dt - \\
& \int_{t_1}^{t_2} \left[ \int_{\gamma L}^L (-EI + (e_0 a)^2 p) \frac{\partial^3 v_2(z, t)}{\partial z^3} \delta \frac{\partial v_2(z, t)}{\partial z} dz \right] dt = \\
& \int_{t_1}^{t_2} \left[ (-EI + (e_0 a)^2 p) \frac{\partial^2 v_2(z, t)}{\partial z^2} \delta \frac{\partial v_2(z, t)}{\partial z} \right]_{\gamma L}^L dt - \\
& \int_{t_1}^{t_2} \left[ (-EI + (e_0 a)^2 p) \frac{\partial^3 v_2(z, t)}{\partial z^3} \delta v_2(z, t) \right]_{\gamma L}^L dt + \\
& \int_{t_1}^{t_2} \left[ \int_{\gamma L}^L (-EI + (e_0 a)^2 p) \frac{\partial^4 v_2(z, t)}{\partial z^4} \delta v_2(z, t) dz \right] dt; \tag{A4}
\end{aligned}$$

and

$$\begin{aligned}
& \int_{t_1}^{t_2} \left[ \int_0^{\gamma L} (e_0 a)^2 \rho A \frac{\partial^2 v_1(z, t)}{\partial t^2} \delta \frac{\partial^2 v_1(z, t)}{\partial z^2} dz \right] dt = \\
& \int_{t_1}^{t_2} \left[ (e_0 a)^2 \rho A \frac{\partial^2 v_1(z, t)}{\partial t^2} \delta \frac{\partial v_1(z, t)}{\partial z} \right]_0^{\gamma L} dt - \\
& \int_{t_1}^{t_2} \left[ \int_0^{\gamma L} (e_0 a)^2 \rho A \frac{\partial^3 v_1(z, t)}{\partial t^2 \partial z} \delta \frac{\partial v_1(z, t)}{\partial z} dz \right] dt = \\
& \int_{t_1}^{t_2} \left[ (e_0 a)^2 \rho A \frac{\partial^2 v_1(z, t)}{\partial t^2} \delta \frac{\partial v_1(z, t)}{\partial z} \right]_0^{\gamma L} dt - \\
& \int_{t_1}^{t_2} \left[ (e_0 a)^2 \rho A \frac{\partial^3 v_1(z, t)}{\partial t^2 \partial z} \delta v_1(z, t) \right]_0^{\gamma L} dt + \\
& \int_{t_1}^{t_2} \left[ \int_0^{\gamma L} (e_0 a)^2 \rho A \frac{\partial^4 v_1(z, t)}{\partial t^2 \partial z^2} \delta v_1(z, t) dz \right] dt; \\
\\
& \int_{t_1}^{t_2} \left[ \int_{\gamma L}^L (e_0 a)^2 \rho A \frac{\partial^2 v_2(z, t)}{\partial t^2} \delta \frac{\partial^2 v_2(z, t)}{\partial z^2} dz \right] dt = \\
& \int_{t_1}^{t_2} \left[ (e_0 a)^2 \rho A \frac{\partial^2 v_2(z, t)}{\partial t^2} \delta \frac{\partial v_2(z, t)}{\partial z} \right]_{\gamma L}^L dt - \\
& \int_{t_1}^{t_2} \left[ \int_{\gamma L}^L (e_0 a)^2 \rho A \frac{\partial^3 v_2(z, t)}{\partial t^2 \partial z} \delta \frac{\partial v_2(z, t)}{\partial z} dz \right] dt = \\
& \int_{t_1}^{t_2} \left[ (e_0 a)^2 \rho A \frac{\partial^2 v_2(z, t)}{\partial t^2} \delta \frac{\partial v_2(z, t)}{\partial z} \right]_{\gamma L}^L dt - \\
& \int_{t_1}^{t_2} \left[ (e_0 a)^2 \rho A \frac{\partial^3 v_2(z, t)}{\partial t^2 \partial z} \delta v_2(z, t) \right]_{\gamma L}^L dt + \\
& \int_{t_1}^{t_2} \left[ \int_{\gamma L}^L (e_0 a)^2 \rho A \frac{\partial^4 v_2(z, t)}{\partial t^2 \partial z^2} \delta v_2(z, t) dz \right] dt; \tag{A5}
\end{aligned}$$